




Synthesis and evaluation of a tri-armed molecular receptor for recognition of mercury and cyanide toxicants

Har Mohindra Chawla, Mohammad Shahid, Lakhbeer Singh Arora & Bhawna Uttam


To cite this article: Har Mohindra Chawla, Mohammad Shahid, Lakhbeer Singh Arora & Bhawna Uttam (2016): Synthesis and evaluation of a tri-armed molecular receptor for recognition of mercury and cyanide toxicants, *Supramolecular Chemistry*, DOI: [10.1080/10610278.2016.1175567](https://doi.org/10.1080/10610278.2016.1175567)

To link to this article: <http://dx.doi.org/10.1080/10610278.2016.1175567>

 View supplementary material 

 Published online: 18 May 2016.

 Submit your article to this journal 

 Article views: 29

 View related articles 

 View Crossmark data 

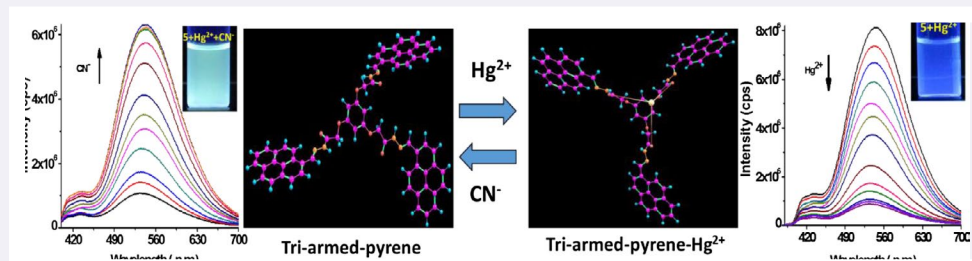
Synthesis and evaluation of a tri-armed molecular receptor for recognition of mercury and cyanide toxicants

Har Mohindra Chawla, Mohammad Shahid, Lakhbeer Singh Arora and Bhawna Uttam

Department of Chemistry, Indian Institute of Technology Delhi, New Delhi, India

ABSTRACT

A tri-armed-pyrene-linked molecular receptor, **5** has been designed, synthesised and evaluated for ionic recognition. It has been observed that the synthesised molecular receptor can recognise mercury and cyanide ions through a change in colour, UV-Vis and fluorescence intensity. The binding stoichiometry of the receptor and these ionic species has been found to be 1:1 through Job's plots, Benesi-Hildebrand plots and isothermal titration calorimetry (ITC).



ARTICLE HISTORY

Received 3 November 2015
Accepted 4 April 2016

KEYWORDS

Tri-armed molecular receptor; mercury; cyanide; pyrene; isothermal titration calorimetry

1. Introduction

The development of multi-armed artificial receptors for recognition of toxic ionic species is an important area of active chemical research (1, 2). Multi-armed (e.g. tripodal) receptors are more advantageous than monopodal and bipodal receptors as they offer better chelating opportunities through apparent convergence of functionalities that can wrap the target toxicant with rigid arms of the receptor (3–6). Till date, only a limited number of multi-armed anion and cation receptors have been reported (3, 7). For example, tripodal receptors have been examined for the detection of ammonium ions (8) due to their potential to assume tetrahedral geometric fit through convergence of functional groups present in the designed receptor. Likewise multi-armed receptors for anions have also been reported, e.g. a tri-armed azo receptor for detection of fluoride (2). Reinhoudt et al. (3, 7) and Ghosh et al. (7) have designed multi-armed receptors for phosphate ions. A few multi-armed receptors have also been developed for the detection of mercury and other toxicants in solution and the vapour phase (7, 8). Some of the receptors examined for mercury ions include those present in the tripodal rhodamine (7), nitrobenzofuran (7),

quinolone (7) and azobenzene (7). There appears to be no report on multi-armed receptors for simultaneous recognition of both mercury and cyanide toxicants.

Mercury ions are extremely poisonous and their action is accumulative with potentially greater damage to human health (9–11). Mercury vapour exposure can lead to brain damage, kidney failure and cognitive and motion disorders (12). Methyl mercury enhances its lipid solubility to yield extremely toxic and damaging species for the central nervous system (13).

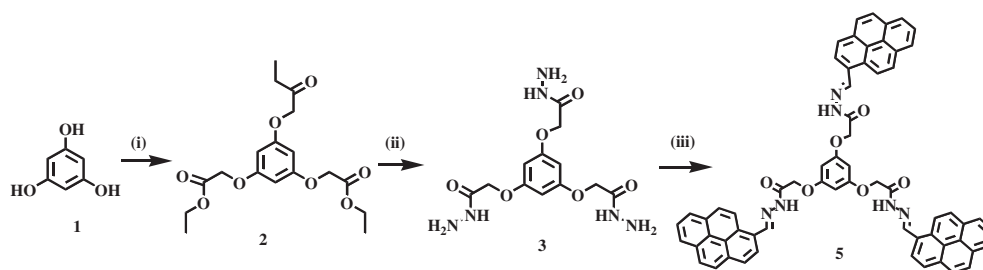
Likewise, cyanide ions can affect the central nervous system as well as cardiac, endocrine and metabolic pathways. Perhaps the most cited adverse effect of cyanide is its inhibition of respiration and terminal oxidase (cytochrome oxidase) activity in the mitochondrial respiratory chain. Cyanide ion, though extensively used in electroplating, plastics, gold and silver extraction, tanning and other metallurgical operations (14), is also a potent chemical warfare agent. There is a need for development of molecular receptors for fast detection of cyanide releasing toxicants.

We report herein a new tri-armed molecular receptor (5) which can simultaneously recognise both mercury and

cyanide toxicants selectively through a change in colour, UV-Vis and fluorescence spectrum. It induces profound quenching of fluorescence intensity on interaction with mercury ions, while it causes enhancement of fluorescence intensity on interaction with CN^- ions. **5**- Hg^{2+} complex is able to selectively recognise CN^- ions in semi aqueous medium with a high association constant and favourable response time. Though binding of receptor seems to be complex, isothermal calorimetric titrations suggest that the recognition process involves non-covalent binding of the receptor and the toxicant.

2. Results and discussion

1,3,5-Trihydroxy benzene (**1**) on acylation with ethyl bromoacetate in the presence of K_2CO_3 and KI gave **2** in 80% yield (Scheme 1). On stirring with hydrazine hydrate in ethanol at room temperature, **2** gave **3** as an off-white solid in 91% yield. Subsequent reaction with 1-pyrenecarboxaldehyde in ethanol – acetic acid yielded **5** as a yellow solid in 60% yield. Full characterisation of **5** was accomplished through spectral and analytical data (Figures S1–7).



Scheme 1. (i) Ethyl bromo acetate/ K_2CO_3 /MeCN/ Δ , (ii) hydrazine hydrate/EtOH/stirring/room temperature, (iii) 1-pyrenecarboxaldehyde (**4**)/EtOH/AcOH/ Δ .

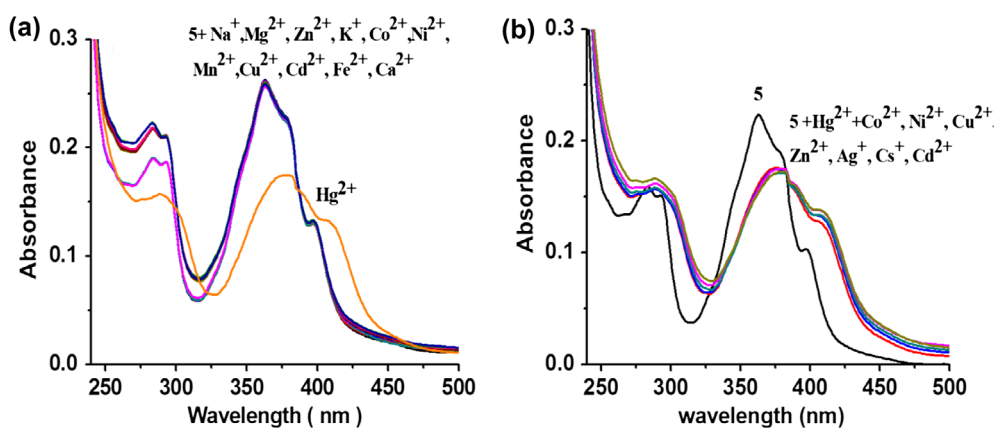


Figure 1. (Colour online) (a) Interaction of **5** ($10\ \mu\text{M}$) with different metal ions and (b) interference of different metal ions (20 equiv) in the analysis of mercury ions in aqueous-MeCN (30%).

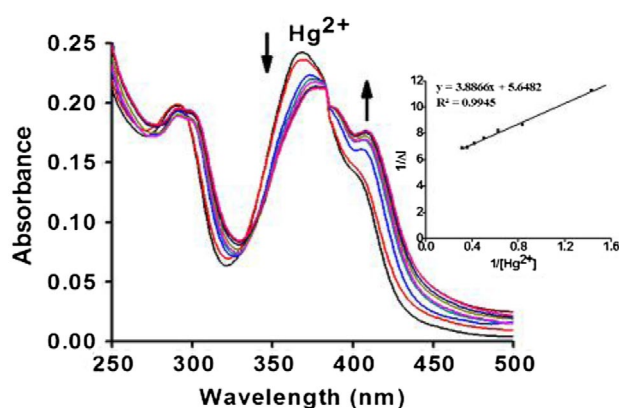


Figure 2. (Colour online) Absorption titrations spectra of **5** ($10\ \mu\text{M}$) with Hg^{2+} (0–3.2 equiv) in aqueous-MeCN (30%). Inset shows Benesi–Hildebrand plot obtained for 1:1 stoichiometry.

2.1. Interaction of tri-armed-pyrene receptor (**5**) with metal ions

2.1.1. UV-visible spectral studies

The ability of **5** for ionic recognition of species was assessed by UV-visible spectroscopy. For this purpose a $10\text{-}\mu\text{M}$ solution of **5** in 30% aqueous-acetonitrile was prepared (absorption maxima at $365\ (\epsilon = 26,181\ \text{M}^{-1}\ \text{cm}^{-1})$ and $285\ \text{nm}\ (\epsilon = 21,633\ \text{M}^{-1}\ \text{cm}^{-1})$). The changes in the spectrum

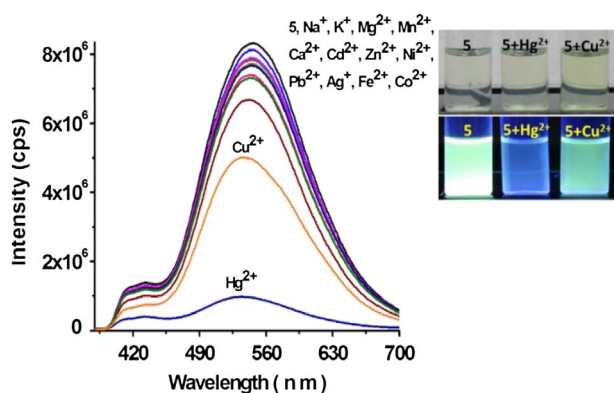


Figure 3. (Colour online) Interaction of **5** (10 μM) with various metal ions (20 equiv) in aqueous-MeCN (30%) revealing a profound quenching on addition of mercury ions. Other similar ions have insignificant quenching effects.

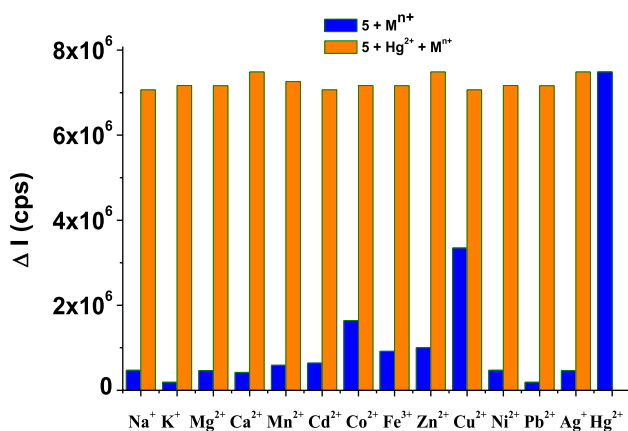


Figure 4. (Colour online) Bar diagram illustrates the change in fluorescence intensity of **5** (blue colour) and a complex, **5** + Hg^{2+} (orange colour) upon addition of tested metal ions (30 equiv) in aqueous-MeCN (30%).

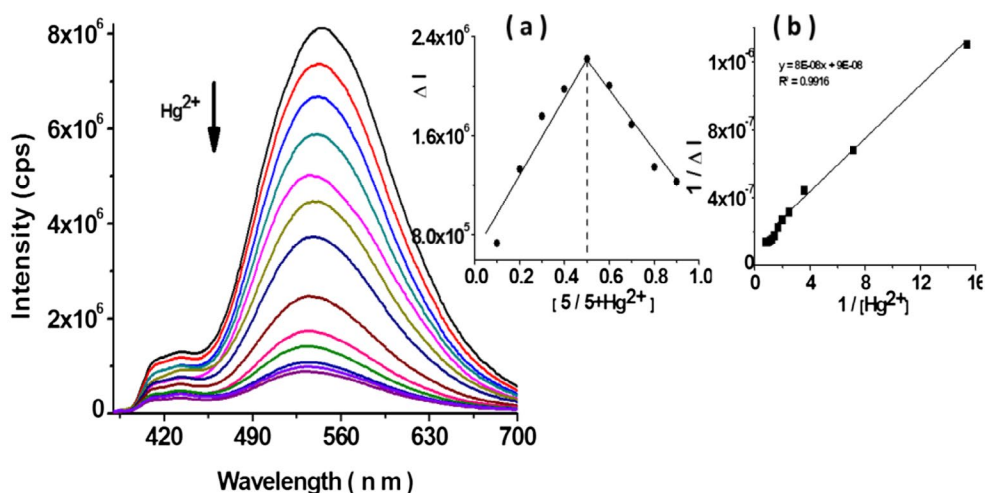


Figure 5. (Colour online) Emission titration spectra of **5** (10 μM) with Hg^{2+} (0–4 equiv) in aqueous-MeCN. Inset: (a) Job's plot and (b) Benesi-Hildebrand plot.

on addition of different metal ions (Na^+ , K^+ , Mg^{2+} , Ca^{2+} , Co^{2+} , Ni^{2+} , Cu^{2+} , Zn^{2+} , Mn^{2+} , Pb^{2+} , Hg^{2+} , Ag^+ , Cs^+ , Cd^{2+} , Fe^{3+} in the form of their nitrate salts) was monitored carefully. No change was noticed in the UV spectrum except when mercury ions were added to the solution of **5** when a bathochromic shift (~ 15 nm) was observed with appearance of a new absorption maxima at 380 nm with a shoulder at 408 nm (Figure 1(a)). In order to understand the metal ion selectivity, interference studies were carried out by addition of competitive metal ions (20 equiv) to a solution of **5** containing Hg^{2+} ions. A profound selectivity for the Hg^{2+} ions was observed over other ionic interferences (Figure 1(b)).

Gradual addition of Hg^{2+} ions (0–3.2 equiv) led to a decrease in absorbance of band at 365 nm with appearance of a new band at 380 nm with a shoulder at 408 nm and an isosbestic points at 384 and 332 nm. The formation of tacit isosbestic points indicated that a new species was formed in the solution (Figure 2). The Job's plot revealed stoichiometry to be 1:1 for which association constant was determined by modified Benesi-Hildebrand method (15) as $1.45 \times 10^5 \text{ M}^{-1}$ by utilising Equation (1),

$$1/(l - l_o) = 1/(l - l_f) + 1/K(l - l_f) [\text{Hg}^{2+}] \quad (1)$$

where K is the association constant, l is absorbance of free receptor **5**, l_o is the observed absorbance of complex, **5**– Hg^{2+} and l_f is the absorbance at saturation.

2.1.2. Fluorescence spectral studies

When **5** (10 μM) was excited at 365 nm, it led to an emission band at 545 nm along with a weak band at 420 nm in aqueous acetonitrile (30%). The emission band appearing at 420 nm could be attributed to pyrene monomeric

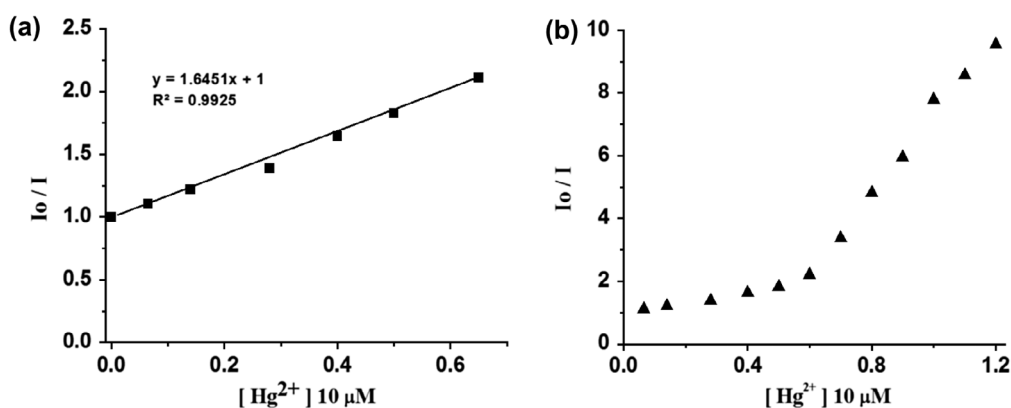


Figure 6. (Colour online) Stern–Volmer graphs for **5** (10 μM) with Hg^{2+} metal ions in aqueous-MeCN (30%).

unit present in the probe, while the band at 545 nm could be assigned to the intramolecular excimer emission and π – π stacking of pyrene units. This was ascertained by the observation that on dilution of **5** (1–10 μM), the emission band remained unchanged at 545 nm (Figure S8). Upon addition of various metal ions (as their nitrate salts), the emission band at 545 nm showed efficient fluorescence quenching only with Hg^{2+} ions (~88% quenching) (Figure 3).

A small fluorescence quenching observed when **5** was interacted with Cu^{2+} ions (~38% quenching) could be considered less significant as none of the other transition metals ions interfered in the detection of mercury in aqueous medium. The quenching effects could be attributed to enhanced spin–orbit coupling and electron transfer mechanisms, respectively (16). The other tested metal ions did not induce any significant change. The interference experiments established reinforced impressive selectivity for Hg^{2+} ions over other metal ions (Figures 4 and S9).

In order to evaluate the association constant, emission spectroscopic titrations were performed (Figure 5). It was determined that the emission maxima continuously decreased in its fluorescence intensity and the spectrum shifted towards blue region on gradual addition of Hg^{2+} ions (0–4 equiv) with a band appearing at 531 nm. Analysis of interaction through Job's plot, revealed a 1:1 stoichiometry between **5** and Hg^{2+} ions and association constant was estimated by utilising Equation (1) as $1.13 \times 10^5 \text{ M}^{-1}$. The detection limit of mercury ion was found to be 0.11 μM (Figure S10, detailed given in ESI).

The observed fluorescence quenching at 545 nm was estimated by obtaining the Stern–Volmer (S–V) plot between the intensity ratio, I_0/I and concentration of Hg^{2+} ions (Figure 6) using Stern–Volmer Equation (2) in which an almost straight line ($R^2 = 0.9921$) was observed up to 0.65 equiv of Hg^{2+} ions with a quenching constant of $K_{\text{S-V}} = 164,510 \text{ M}^{-1}$ as calculated from

$$F_0 / F = 1 + K_{\text{S-V}} [Q] \quad (2)$$

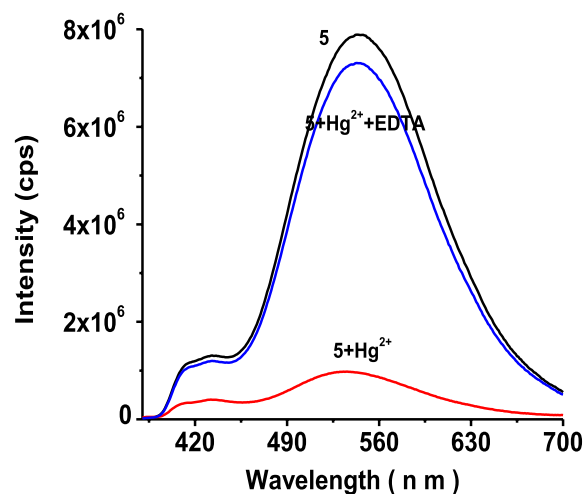


Figure 7. (Colour online) Reusability of **5**, 5-Hg^{2+} on treatment with EDTA in aqueous-MeCN (30%).

where, F_0 and F is fluorescence intensity of tri-armed receptor in the absence and presence of quencher (Hg^{2+}), respectively. $K_{\text{S-V}}$ is quenching constant and Q is the quencher concentration.

The Stern–Volmer plots were linear up to 0.65 equiv of Hg^{2+} but it became a non-linear plot with an upward curvature at 1.2 equiv of mercury. This indicated that both static (collisional) as well as dynamic (formation of non-fluorescent ground state complex) quenching might be governing the interaction of metal ions and the receptor (17).

The reversibility of interaction of receptor and Hg^{2+} ions was analysed by adding a strong chelating reagent, disodium ethylene diamine tetra acetate (EDTA, 50 equiv) to a solution of plausible 1:1 complex 5-Hg^{2+} (Figure 7). The quenched emission band of $5 + \text{Hg}^{2+}$ was observed to disappear with the generation of original band at respective wavelength due to the formation of a strong EDTA-Hg^{2+} complex in the medium. This experiment suggested the reversible nature of complexation between mercury ions and **5** and the observations could be considered to be a part of a repeat cycle.

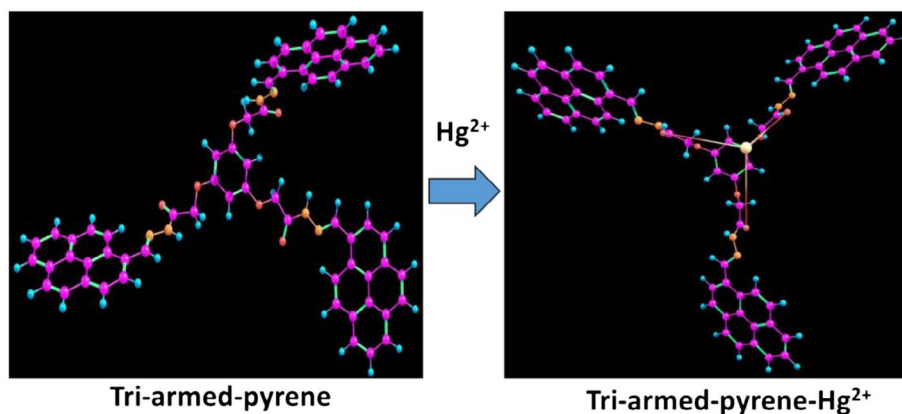


Figure 8. (Colour online) DFT structure of **5** and its probable complex with Hg^{2+} .

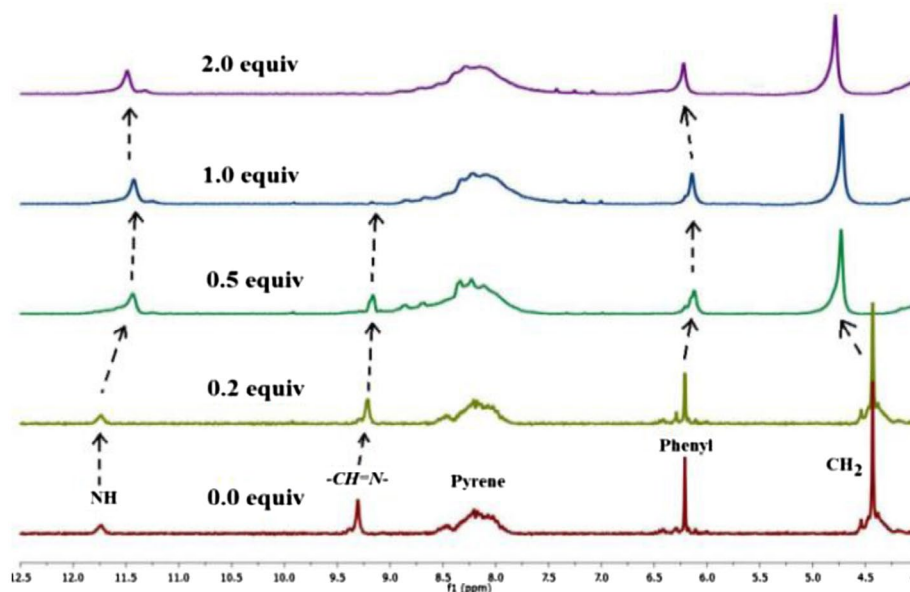


Figure 9. (Colour online) ^1H NMR titration spectra of **5** (2.23×10^{-2} M) with Hg^{2+} (0–2 equiv) as their nitrate salt in $\text{DMSO}-d_6$.

2.2. Mechanism of interaction of **5** and Hg^{2+}

Geometry optimisation of **5** and its plausible complex (**5** + Hg^{2+}) was examined through density functional calculations (DFT) employing a basis set B3LYP/6-31G and B3LYP/LANL2DZ using Gaussian 03 programme, respectively (18). The optimised structure showed that two pyrene moieties of **5** are closer which on interaction with Hg^{2+} ions get away from each other as shown in Figure 8.

The probable mechanism of interaction of **5** and Hg^{2+} was investigated by ^1H NMR titration of **5** in the presence of different concentrations of Hg^{2+} ions (0.2, 0.5, 1 and 2 equiv) as presented in Figure 9. Upon addition of 0.2–2.0 equiv of Hg^{2+} ions to **5**, a significant upfield shift ($\Delta\delta = 0.22$ and 0.41 ppm) was observed in the resonances of amide and aldimine protons, respectively, while resonances of pyrene ring protons became broad. These

observations suggested that Hg^{2+} ions may be coordinated to both amide and aldimine functions present in **5**.

Studies on binding of 5 with Hg^{2+} through isothermal titration calorimetry (ITC): Thermodynamic parameters for the host–guest complex formation was further investigated by isothermal titration calorimetry (ITC) on interaction of **5** and Hg^{2+} at 25°C in aqueous-MeCN (30%, v/v) (8). The binding isotherm again showed a 1:1 stoichiometry for complexation between **5** and Hg^{2+} ions (Figure 10) with formation constant as $1.15 \times 10^4 \text{ M}^{-1}$. The enthalpy change ΔH° was measured as $-1.545 \times 10^6 \pm 1.704 \times 10^4 \text{ cal/mol}$ and entropy changes ΔS° is $-5.16 \times 10^3 \text{ cal/mol/deg}$ for the formation of the **5**– Hg^{2+} complex. The overall binding enthalpy seems to originate from non-covalent interactions between **5** and Hg^{2+} ions with loss of entropy.

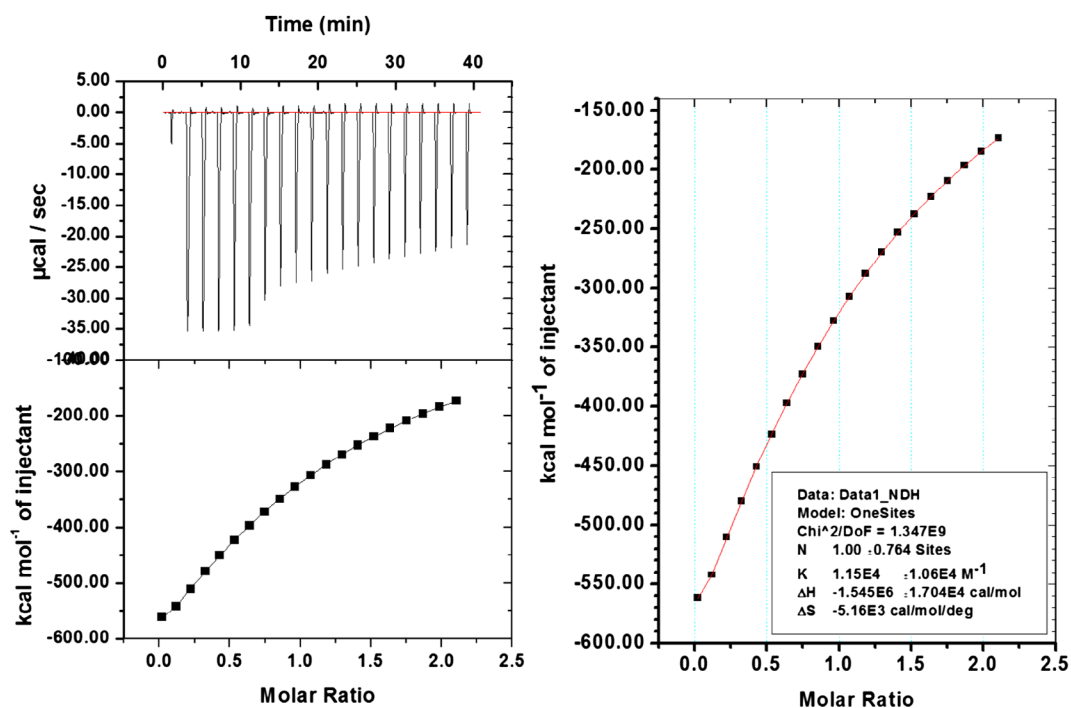


Figure 10. (Colour online) Interaction of 5 with Hg^{2+} ions in aqueous-MeCN (30%, v/v) at 25 °C.

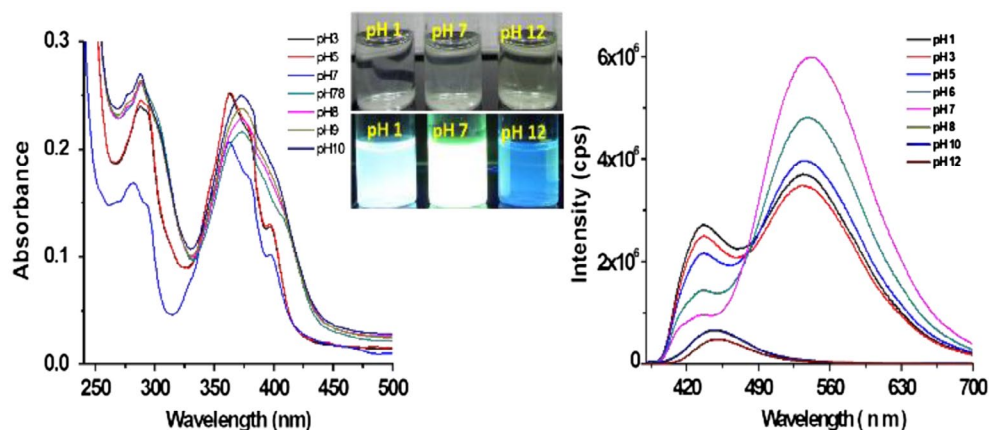


Figure 11. (Colour online) (a) Absorption and (b) emission behavior of 5 at different pHs.

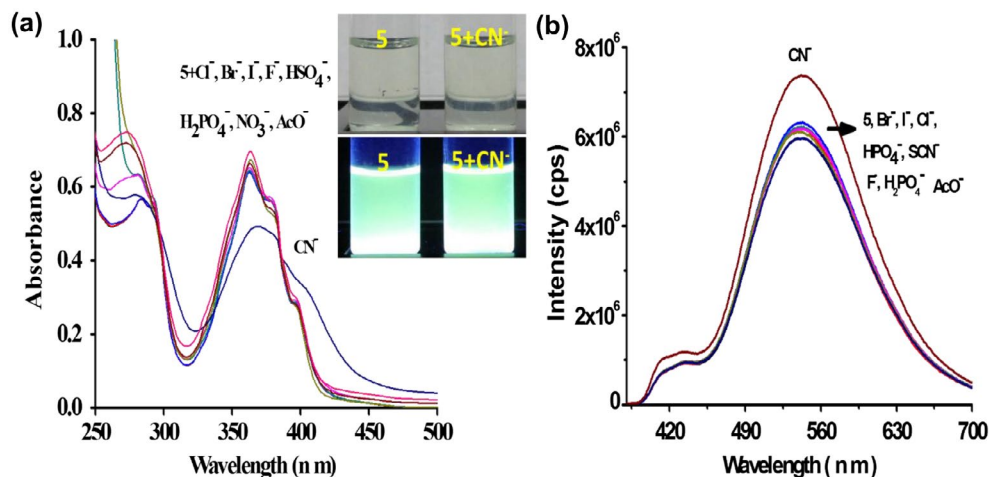


Figure 12. (Colour online) Interaction of 5 (10 μM) with different anions (20 equiv) in aqueous-MeCN (30%).

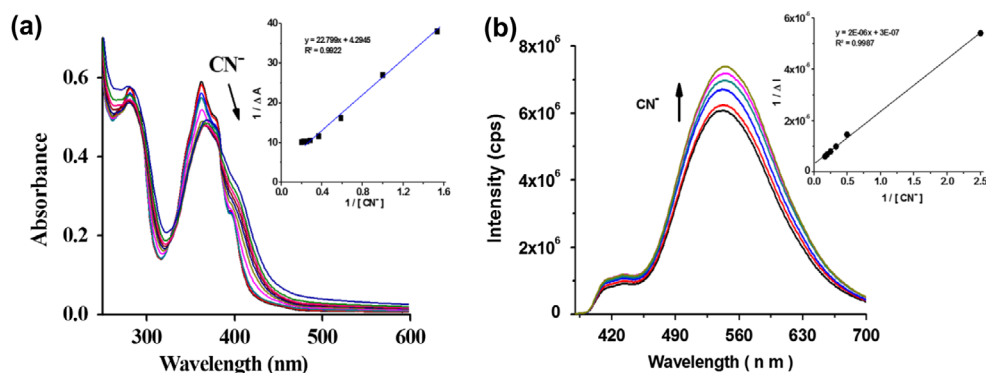


Figure 13. (Colour online) (a) Absorption and (b) emission titration spectra of **5** (10 μM) on addition of CN^- (0–5 equiv) in aqueous-MeCN (30%). Inset shows Benesi–Hildebrand plot obtained for 1:1 stoichiometry.

2.3. Spectral behaviour of **5** at different pHs

The absorption and emission spectra of **5** at different pHs were also studied. It was observed that in the acidic medium, pH (7–12) a hyperchromic shift was observed. In the basic medium, a bathochromic shift along with hyperchromism was noticed (Figure 10). The fluorescence behaviour of **5** when examined as a function of pH under similar experimental conditions (Figure 11) revealed that relative fluorescence intensity of **5** increased from pH 1 to 7 while considerable fluorescence quenching occurred under pH range of 8–12, respectively. The observed relative emission intensity was low in the acidic medium (<pH 7) and could be attributed to protonation of carbonyl group, while under basic conditions (>pH 7) the fluorescence intensity seemed to get fully quenched possibly because of deprotonation of amide functions.

2.4. Anion recognition through **5**

A survey of the literature indicates that **5** could also be used as a receptor for anions as **5** contains a number of amide groups that could confer appropriate acidity to exhibit sensitive optical properties. It was observed that the absorption spectra of **5** could be modulated significantly when CN^- ions were added while no change was noticed on addition of other anions (Cl^- , Br^- , I^- , F^- , HSO_4^- , H_2PO_4^- , SCN^- , AcO^- and CN^- (as their tetrabutylammonium salts) at 20 equiv concentration. A bathochromic shift (~ 7 nm) was noticed with a new absorption peak at 372 nm on addition of CN^- ions (Figure 12(a)). Detailed analysis revealed that addition of different anions (20 equiv) exhibited fluorescence enhancement upon interaction with only CN^- ions in the emission spectrum, whereas related anions like F^- , H_2PO_4^- and AcO^- showed efficient fluorescence quenching in acetonitrile. Tri-armed receptor **5** did not exhibit any selectivity for anions in acetonitrile solution (Figure S11).

In aqueous–acetonitrile solutions, **5** exhibited a fluorescence enhancement on interaction with only cyanide

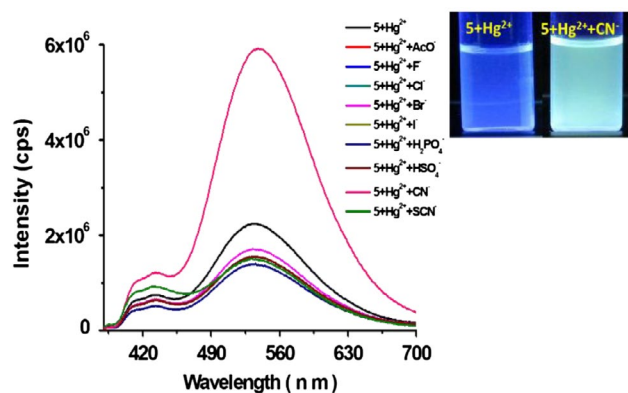


Figure 14. (Colour online) Interaction studies of **5**– Hg^{2+} complex (10 μM) with various anions (20 equiv) in aqueous-MeCN (30%).

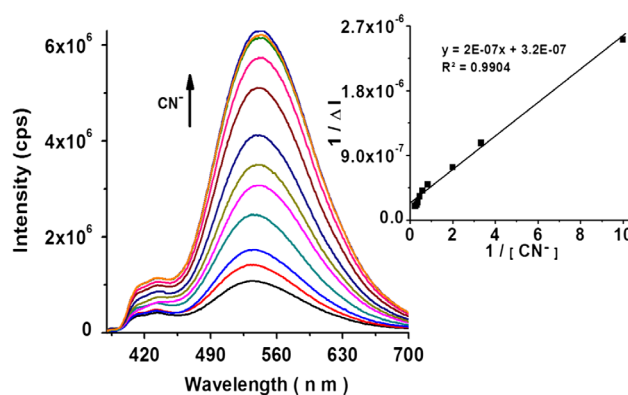


Figure 15. (Colour online) Emission titration spectra of **5**– Hg^{2+} complex with CN^- (0–4 equiv) in aqueous-MeCN (30%). Inset shows Benesi–Hildebrand plot.

ions possibly through H-bond interactions with the amide functions present in **5** (Figure 12(b)) (19).

The binding affinity of **5** for CN^- was examined by absorption and emission spectral titrations (Figure 13). Gradual addition of CN^- (0–5 equiv) to a solution of **5**, led to a decrease in the absorbance at 365 nm with the formation of a new band at 370 nm with an isosbestic point

at 382 nm. Similarly in the emission spectra, addition of CN^- ions (0–5 equiv) led to increase in fluorescence intensity of **5**. Job's plot analysis revealed a 1:1 stoichiometry for the complexation of **5** with CN^- (19). The association constant estimated from non-linear fitting of absorption and emission titration data using Equation (1) was found to be $K_{\text{assos}} = 1.8 \times 10^4$ and $1.5 \times 10^4 \text{ M}^{-1}$, respectively (inset of Figure 13).

The probable mechanism of interaction of **5** and CN^- was investigated by ^1H NMR titration. Though addition of CN^- ions (1 equiv) to the molecular receptor **5** in deuterated dimethyl sulfoxide, led to the broadening of all signals but a significant downfield shift of NH signal at 1 equiv and total disappearance of amide protons at 2 equiv addition of cyanide indicates strong interaction of cyanide with amide protons as expected (Figure S12).

2.5. Ion recognition properties of 5– Hg^{2+} complex

The optical behaviour of **5**– Hg^{2+} complex (10 μM) was examined in the presence of different anions in aqueous-MeCN solution (30%). Upon addition of different anions (10 equiv) such as, F^- , Cl^- , Br^- , I^- , SCN^- , H_2PO_4^- , CN^- , AcO^- , HSO_4^- (as their tetrabutylammonium/sodium salts) to a solution of **5**– Hg^{2+} , significant changes in the optical properties were observed on interaction with CN^- ions only. A complete restoration of the emission spectra of **5** was observed (Figure 14).

The binding affinity of a complex, **5**– Hg^{2+} with CN^- ions was estimated by performing emission titration experiments (Figure 15). On sequential addition of CN^- (0–4 equiv) to a solution of **5**– Hg^{2+} , the intensity of emission band centred at 530 nm got enhanced. It was considered significant to observe that the colour of the solution could be distinguished by naked eye. Fluorescence titration could be utilised to estimate binding constant of CN^- ions for a complex, **5**– Hg^{2+} using Equation (1) as $1.61 \times 10^5 \text{ M}^{-1}$. The detection limit of **5**– Hg^{2+} complex for CN^- ion was estimated to be 0.7 μM , which is lower than the maximum permissible level of cyanide in drinking water (1.9 ppm).

Though final resolution of speculative nature of binding mechanism is possible through X-ray diffraction analysis, single crystals suitable for X-ray analysis, however, could not be grown at this point of time.

3. Conclusion

A new tri-armed receptor **5** has been synthesised and evaluated for recognition of cations and anions. It has been observed that **5** exhibits an intramolecular excimer fluorescence due to π – π interaction of pyrene ring. The intensity of fluorescence of receptor **5** is quenched by

Hg^{2+} and enhanced by CN^- ions in an aqueous–acetonitrile solvent. The Job's plot, Stern–Volmer plots, Benesi–Hildebrand treatment and isothermal titration calorimetry data show a 1:1 stoichiometry between **5** and Hg^{2+} ions. Preliminary DFT calculations support this conclusion. The **5**– Hg^{2+} complex can be further utilised for the detection of CN^- ions through metal ion displacement mechanism.

4. Experimental

4.1. Synthesis of compound 2

Compound **2** was synthesised by a minor modification of the previously reported procedure (19, 20). In the present case, to a solution of 1, 3, 5-trihydroxy benzene (0.25 g, 1.98 mmol), K_2CO_3 (1.09 g, 7.89 mmol) and KI (a pinch) in anhydrous acetonitrile, ethyl bromoacetate (0.76 ml, 4.59 mmol) was added. The reaction mixture was refluxed overnight and the progress of the reaction was monitored by thin layer chromatography. The reaction mixture was filtered and the solvent was evaporated under reduced pressure. The crude product obtained was dissolved in chloroform and washed with water thrice ($3 \times 20 \text{ ml}$). The organic layer was dried over anhydrous Na_2SO_4 . The solvent was evaporated under vacuum to yield **2** as a gummy solid (Yield: 80%). ^1H NMR (300 MHz, CDCl_3): δ (ppm) 6.184 (s, 3H, phenyl), 4.71 (s, 6H, $-\text{OCH}_2\text{CO}$), 4.47 (m, 6H, COCH_2), 1.34 (t, 9H, $-\text{CH}_3$).

4.2. Synthesis of compound 3

To a solution of compound **2** (0.50 g, 1.6 mmol) in ethanol, hydrated hydrazine (0.52 g, 16.3 mmol, 99%) was added and the reaction mixture was stirred at room temperature for 2 h. The precipitate obtained was filtered and washed with cold water and dried to get **3** as off white solid. (Yield: 91%). Mp. 236–240 °C. ^1H NMR (300 MHz, CDCl_3): δ (ppm) 9.22 (s, 3H, $-\text{CONH}$), 6.18 (s, 3H, phenyl), 4.47 (s, 6H, $-\text{OCH}_2\text{CO}$), 3.59 (s, 6H, $-\text{NH}_2$); FT-IR (KBr, cm^{-1}): 3322 cm^{-1} (N–H), 2917 cm^{-1} ($-\text{CH}_2$ asym. stretch, Alkyl), 2869 cm^{-1} (CH_2 , sym. stretch), 1669 cm^{-1} ($-\text{CONH}$), 1611 cm^{-1} (C=C, aromatic), 1477 cm^{-1} (C–C stretch in ring).

4.3. Synthesis of compound 5

To a suspension of **3** (0.10 g, 0.29 mmol) in ethanol containing acetic acid (0.1 ml), 1-pyrenecarboxaldehyde, **4** (0.21 g, 0.91 mmol) was added and the reaction mixture was refluxed overnight. The precipitate obtained was filtered and washed with cold ethanol to yield **5** as a yellow solid (Yield: 60%). Mp. 275–280 °C (charring); ^1H NMR (300 MHz, $\text{DMSO}-d_6$): δ (ppm) 11.74 (s, 3H, NH), 9.31 (s, 3H, $\text{CH}=\text{N}$), 8.46 (m, 27H), 6.17 (s, 3H, phenyl), 4.53 (s, 6H, COCH_2); ^{13}C NMR (75 MHz, CDCl_3): δ (ppm) 168.8, 166.8, 159.9, 136.3, 131.4, 130.6, 128.9, 128.6, 127.6, 126.3, 125.4, 125.3, 124.2, 123.0,

121.6, 95.3, 66.8; HR-MS calculated for $[C_{63}H_{42}O_6N_6 + H]^+$ at m/z 979.3208 and found at m/z 979.3238; FT-IR (KBr, cm^{-1}) 3324 (N-H), 2920 (C-H, Alkane), 1672 (CO-NH), 1610 (C=C), 1182 (C-N), 1080 (C-O-C).

Supplemental material

Supplemental data for this article can be accessed online here: <http://dx.doi.org/10.1080/10610278.2016.1175567>.

Acknowledgements

The authors thank SERB, a unit of the Department of Science and Technology (DST), New Delhi for financial support vide sanction No. SB/FT/CS-010/2013 and financial assistance from MoEF, MoRD and MoFPI (Govt. of India) for the project on fruwash technology is gratefully acknowledged. The authors thank Professor Shashank Deep and Mr Vinay Kumar for their help in securing isothermal titration calorimetry data.

Disclosure statement

No potential conflict of interest was reported by the authors.

References

- (1) Berocal, M.J.; Cruz, A.; Badrand, L.I.H.A.; Bachas, G.. *Anal. Chem.* **2000**, *72*, 5295–5299.
- (2) Reinoso-Garcia, M.M.; Dijkman, A.; Verboom, W.; Reinhoudt, D.N.; Malinoswka, E.; Wojciechowska, D.; Pietrzak, M.; Selucky, P. *Eur. J. Org. Chem.* **2005**, *2005*, 2131–2138; Mahapatra, A.K.; Manna, S.K.; Sahoo, P. *Talanta* **2011**, *85*, 2673–2680.
- (3) Kuswandi, B.; Nuriman; Verboom, W.; Reinhoudt, D.N. *Sensors* **2006**, *6*, 978–1017.
- (4) Sato, K.; Arail, S.; Yamagishi, T. *Tetrahedron Lett.* **1999**, *40*, 5219–5222.
- (5) Ballester, P.; Costa, A.; Deyii, P.M.; Vega, M.; Morey, J. *Tetrahedron Lett.* **1999**, *40*, 171–174.
- (6) Fan, A.L.; Hong, H.K.; Valiyaveetil, S.; Vittal, J.J. *J. Supramol. Chem.* **2002**, *2*, 247–254.
- (7) Valiyaveetil, S.K.; Engbersen, J.F.J.; Verboom, W.; Reinhoudt, D.N. *Angew. Chem. Int. Ed. Engl.* **1993**, *32*, 900–901; Ravikumar, I.; Lakshminarayanan, P.S.; Arunachalam, M.; Suresh, E.; Ghosh, P. *Dalton Trans.* **2009**, 4160–4168; Lakshminarayanan, P.S.; Ravikumar, I.; Suresh, E.; Ghosh, P. *Chem. Commun.* **2007**, 5214–5216; Zenga, X.; Donga, L.; Wua, C.; Mua, L.; Xuea, S.-F.; Tao, Z. *Sens. Actuat. B* **2009**, *141*, 506–510; Lee, M.H.; Wu, J.-S.; Lee, J.W.; Jung, J.H.; Kim, J.S. *Org. Lett.* **2007**, *9*, 2501–2504; Nuriman; Kuswandi, B.; Verboom, W. *Sens. Lett.* **2011**, *9*, 1–7; Ahamed, N.; Ghosh, P. *Dalton Trans.* **2011**, *40*, 12540–12547; Sánchez, G.; Curiel, D.; Ratera, I.; Tárraga, A.; Veciana, J.; Molina, P. *Dalton Trans.* **2013**, 42, 6318–6326; Kaur, N.; Singh, N.; Cairns, D.; Callan, J.F. *Org. Lett.* **2009**, *11*, 2229–2232; Zhou, Y.-P.; Liu, E.-B.; Wang, J.; Chao, H.-Y. *Inorg. Chem.* **2013**, *52*, 8629–8637.
- (8) Metzger, A.; Lynch, V.M.; Anslyn, E.V. *Angew. Chem. Int. Ed. Engl.* **1997**, *36*, 862; Niikura, K.; Metzger, A.; Anslyn, E.V. *J. Am. Chem. Soc.* **1998**, *120*, 8533–8534; Kim, S.-G.; Kim, K.-H.; Jung, J.; Shin, S.K.; Ahn, K.H. *J. Am. Chem. Soc.* **2002**, *124*, 591–596; Ahn, K.H.; Ku, H.-Y.; Kim, Y.; Kim, S.-G.; Kim, Y.K.; Son, H.S.; Ku, J.K. *Org. Lett.* **2003**, *5*, 1419–1422; Kim, S.-G.; Ahn, K.H. *Chem.-Eur. J.* **2000**, *6*, 3399–3403; Chin, J.; Walsdorff, C.; Stranix, B.; Oh, J.; Chung, H.J.; Park, S.-M.; Kim, K. *Angew. Chem. Int. Ed.* **1999**, *38*, 2756–2759; Kim, J.; Kim, S.-G.; Seong, H.R.; Ahn, K.H. *J. Org. Chem.* **2005**, *70*, 7227–7231; Kim, J.; Raman, B.; Ahn, K.H. *J. Org. Chem.* **2006**, *71*, 38–45; Kim, S.-G.; Kim, K.-H.; Kim, Y.K.; Shin, S.K.; Ahn, K.H. *J. Am. Chem. Soc.* **2003**, *125*, 13819–13824.
- (9) Harris, H.H.; Pickering, I.J.; George, G.N. *Science* **2003**, *301*, 1203.
- (10) Weiss, B. *Toxicol. Sci.* **2007**, *97*, 223–225; Lin, Q.; Sun, B.; Yang, Q.-P.; Fu, Y.-P.; Zhu, X.; Wei, T.-B.; Zhang, Y.-M. *Chem. Eur. J.* **2014**, *20*, 11457–11462; Lin, Q.; Lu, T.-T.; Zhu, X.; Sun, B.; Yang, Q.-P.; Weia, T.-B.; Zhang, Y.-M. *Chem. Commun.* **2015**, *51*, 1635–1638; Wei, T.-B.; Gao, G.-Y.; Qu, W.-J.; Shi, B.-B.; Lin, Q.; Yao, H.; Zhang, Y.-M. *Sens. Actuat. B* **2014**, *199*, 142–147; Zhang, Y.M.; Qu, W.J.; Gao, G.Y.; Shi, B.B.; Wu, G.Y.; Wei, T.B.; Lin, Q.; Yao, H. *New J. Chem.* **2014**, *38*, 5075–5080.
- (11) Amin-Zaki, L.; Elhassani, S.; Majeed, M.A.; Clarkson, T.W.; Doherty, R.A.; Greenwood, M. *Pediatrics* **1974**, *54*, 587–595.
- (12) Tchounwou, P.B.; Ayensu, W.K.; Ninashvili, N.; Sutton, D. *Environ. Toxicol.* **2003**, *18*, 149–175.
- (13) Atchison, W.D.; Hare, M.F. *FASEB J.* **1994**, *8*, 622–629.
- (14) Xu, Z.; Chen, X.; Kim, H.N.; Yoon, J. *Chem. Soc. Rev.* **2010**, *39*, 127–137; Wang, F.; Wang, L.; Chen, X.; Yoon, J. *Chem. Soc. Rev.* **2014**, *43*, 4312–4324; Lebeda, F.J.; Deshpande, S.S. *Anal. Biochem.* **1990**, *187*, 302–309.
- (15) Benesi, H.A.; Hildebrand, J.H. *J. Am. Chem. Soc.* **1949**, *71*, 2703–2707; Connors, K.A. *Binding Constant*, 1st ed.; Wiley: New York, NY, **1987**.
- (16) Misra, A.; Shahid, M.; Srivastava, P.; Dwivedi, P. *J. Incl. Phenom. Macrocycl. Chem.* **2011**, *69*, 119–129 and references cited there in.
- (17) Chatwal, M.; Kumar, A.; Gupta, R.D.; Awasthi, S.K. *RSC Adv.* **2015**, *5*, 51678–51681.
- (18) Frisch, M.J.; Trucks, G.W.; Schlegel, H.B. *GAUSSIAN 03, Revision E.01*; Gaussian: Wallingford, CT, **2007**.
- (19) Shahid, M.; Razi, S.S.; Srivastava, P.; Ali, R.; Maiti, B.; Misra, A. *Tetrahedron* **2012**, *68*, 9076–9084; Kim, D.-S.; Chung, Y.-M.; Jun, M.; Ahn, K.H. *J. Org. Chem.* **2009**, *74*, 4849–4854; Lee, D.Y.; Singh, N.; Satyender, A.; Jang, D.O. *Tetrahedron Lett.* **2011**, *52*, 6919–6922; Singh, N.; Jang, D.O. *Org. Lett.* **2007**, *9*, 1991–1994.
- (20) Chawla, H.M.; Shahid, M.; Black, D. StC; Kumar, N. *New J. Chem.* **2014**, *38*, 2763–2765.